Available online at www.sciencedirect.com
ScienceDirect
Nuclear and Particle Physics Proceedings 00 (2022) 1–6
Nuclear and Particle Physics Proceedings

Recent results from Belle II *

Valerio Bertacchi on behalf of the Belle II collaboration[a]

[a]Aix Marseille Univ, CNRS/IN2P3, CPPM, Marseille, France

Abstract

The Belle II experiment at the SuperKEKB energy-asymmetric e^+e^- collider is a substantial upgrade of the B factory facility at the Japanese KEK laboratory. The design luminosity of the machine is $6 \cdot 10^{35}$ cm^{-2}s^{-1} and the Belle II experiment aims to ultimately record 50 ab^{-1} of data, a factor of 50 more than its predecessor. With this data set, Belle II will be able to measure the Cabibbo-Kobayashi-Maskawa (CKM) matrix elements with unprecedented precision and explore flavor physics with B and D mesons, and τ leptons. Belle II has also a unique capability to search for low-mass dark matter and low-mass mediators. In this work, I will review the latest results from Belle II.

Keywords: Belle II, SuperKEKB, B-Factory, Charm, CKM Matrix, CP violation, Time Dependent CP violation, Rare B decays, Dark sector

1. Introduction

Belle II is the general purpose detector that is operated at the second generation B-Factory SuperKEKB. More details about Belle II can be found in Ref. [1, 2].

Belle II started the data taking in 2019, and reached a peak luminosity of $4.7 \cdot 10^{34}$cm^{-2}s^{-1}, which constitutes the world record. The total integrated luminosity collected by Belle II is 424 fb^{-1}. It is almost equivalent to the size of BaBar [3] sample or half of the Belle [4] sample.

2. Charm sector: D^0, D^+, Λ_c^+ lifetime measurements

Charmed hadrons lifetime predictions are challenging because they involve strong-interaction theory at low energy. The predictions rely on effective models, like heavy-quark expansion (HQE) [5], with large uncertainties from high-order corrections. Direct measurements of the charmed hadron lifetimes allow to test these models.

The B-Factories are an optimal environment to perform these measurements, thanks to the large $c\bar{c}$ cross section and the possibility to perform absolute measurements of the lifetimes, without requiring a selection that can bias the lifetime distribution. Moreover the SuperKEKB small interaction region and the Belle II vertex resolution provide strong constraints and improve the precision, compared to previous experiments.

The measurement of D^0 and D^+ lifetimes [6] is performed using $D^{*+} \to D^0(\to K^-\pi^+)\pi^+$ and $D^{*+} \to D^+(\to K^-\pi^+\pi^+)\pi^0$ decays (charge-conjugate decays are implied in the entire manuscript). A data sample equivalent to an integrated luminosity of 72 fb^{-1} is used. The displacement $\vec{L}$ between the production and the decay vertex of the D^0 and D^+ is 200 and 500 μm on average, respectively. The decay time is extracted from the measured displacement projecting the latter on the D momentum $\vec{p}$, $t = m_D\vec{L} \cdot \vec{p}/|\vec{p}|^2$, where m_D is the known mass of the corresponding D meson. The lifetimes are determined from an unbinned maximum-likelihood fit to the 2-dimensional (t, σ_t) distribution, where σ_t is the time uncertainty distribution. The signal region is defined as 1.855 GeV $< m_{K^-\pi^+\pi^+} <$ 1.883 GeV and 1.851 GeV $< m_{K^-\pi^+} <$ 1.878 GeV for D^+ and D^0 respectively. The background contamination is

*Review talk presented at QCD22, 25th International Conference in Quantum Chromodynamics (4-7/07/2022, Montpellier - FR).

Email address: bertacchi@cppm.in2p3.fr (Valerio Bertacchi on behalf of the Belle II collaboration)

estimated as 0.2% and thus neglected in the fit of D^0 channel. The background is modeled using data in the invariant mass sideband for the D^+ channel and fitted simultaneously to the signal resulting in a 9% contamination. The decay time distribution projections are shown in Fig. 1. The result are:

$$\tau_{D^0} = 410.5 \pm 1.1\,(\text{stat}) \pm 0.8\,(\text{syst})\ \text{fs},$$

$$\tau_{D^+} = 1030.4 \pm 4.7\,(\text{stat}) \pm 3.1\,(\text{syst})\ \text{fs}.$$

They are the world's most accurate measurements, in agreement with the world average obtained from the previous measurements ($\tau^{\text{w.a.}}_{D^0} = 410.1 \pm 1.5$ fs, $\tau^{\text{w.a.}}_{D^+} = 1040 \pm 7$ fs [7]).

The measurement of Λ_c lifetime [8] is performed with the same strategy, using the $\Lambda_c^+ \to pK^-\pi^+$ decays. A data sample equivalent to an integrated luminosity of 207.2 fb^{-1} is used. The lifetime is extracted from unbinned maximum-likelihood fit to the 2-dimensional (t, σ_t) distribution, the background model is determined from data in the invariant-mass sideband, where signal window is defined as 2.283 GeV $< m_{pK^-\pi^+} <$ 2.290 GeV, resulting in a 7.5% contamination. The result is:

$$\tau_{\Lambda_c^+} = 203.20 \pm 0.89\,(\text{stat}) \pm 0.77\,(\text{syst})\ \text{fs}.$$

It is the world's most accurate measurement, in agreement with the world average obtained from the previous measurements ($\tau^{\text{w.a.}}_{\Lambda_c^+} = 202.4 \pm 3.1$ fs [7]).

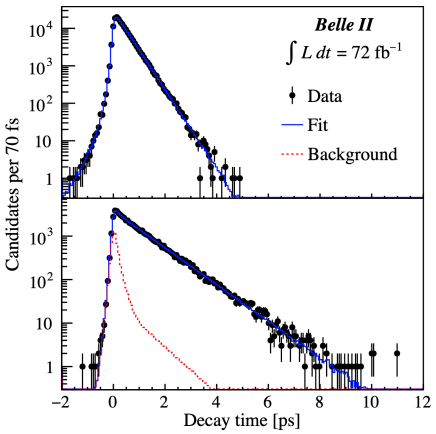

Figure 1: Decay time distribution of (top) $D^0 \to K^-\pi^+$ and (bottom) $D^+ \to K^-\pi^+\pi^+$ candidates in their respective signal regions with fit projections overlaid (from Ref. [6]).

3. CKM Matrix elements measurements

The measurements of the unitarity triangle angles and CKM matrix elements, combined in a global fit, over-constraint the CKM model and therefore can be used as a powerful tool to test the consistency of the Standard Model (SM). Moreover, the CKM matrix elements uncertainties limit the interpretations of rare decays measurements, sensitive to Beyond the Standard Model (BSM) physics.

In this framework one of the topic of interest is the longstanding tension between the inclusive and exclusive determination of $|V_{cb}|$ and $|V_{ub}|$ CKM matrix elements [9]. Currently they both show a 3σ discrepancy between the two determinations.

Belle II investigates this sector performing several measurements of semileptonic B decays as reported in the following sections. Typically these analyses are deployed exploiting the *B-tagging* techniques, which will be introduced in the next section.

3.1. B-tagging at Belle II

The B-tagging techniques are set of reconstruction approaches adopted to identify $\Upsilon(4S) \to B\overline{B}$ events. It is possible to exploit the full knowledge of the initial state in channels with missing energy in the final state to constraint the missing information. First, one of the two B's, called B_{tag}, is reconstructed using some well-known channels. Then the second B, called B_{sig}, is reconstructed using the remaining particles. The identification of the B_{tag}, and the knowledge of the initial $\Upsilon(4S)$ state allow inferring the properties on the B_{sig}, like charge, flavour and momentum.

Different approaches can be used. In the *hadronic tagging*, the B_{tag} is reconstructed using hadronic decays, where the purity is very high despite a lower efficiency due to the small branching fractions. In the *semileptonic tagging* the B_{tag} is reconstructed using semileptonic decays, obtaining higher efficiency thanks to the higher branching fractions, but lower purity because of the missing neutrino(s). In the *inclusive tagging*, the signal is reconstructed first, and then all the tracks and the clusters of the Rest Of the Event (ROE) are used to infer the missing information on the B_{sig}.

In Belle II the most used B-tagging algorithm is the Full Event Interpretation (FEI) [10], an MVA-based tagging algorithm which exploits a hierarchical approach to reconstruct $O(10^4)$ decay chains on the tag side. The efficiencies (purities) are about 0.5% (30%) for the hadronic tag and 2% (10%) for the semileptonic tag.

3.2. Lepton q^2 moments in $B \to X_c\ell\overline{\nu}_\ell$

The HQE can be used to extract $|V_{cb}|$ from the inclusive decay width $\Gamma_{B\to X_c\ell\nu_\ell}$ and spectral moments of lepton- energy and hadron-mass in a model independent way. Unfortunately the proliferation of non-perturbative

matrix elements in the expansion beyond $O(1/m_b^3)$ complicates the extraction of $|V_{cb}|$. A novel method is presented in Ref. [11]. It exploits the reparameterization invariance to reduce to 8 the matrix elements but requires the lepton $q^2 = (p_\ell + p_\nu)^2$ spectral moments.

Belle II measured the first four raw and central q^2 moments of $B \to X_c \ell \overline{\nu}_\ell$ as a function of the lower q^2 threshold, in the range $[1.5, 8.5]$ GeV^2 [12]. A sample equivalent to an integrated luminosity of 62.8 fb^{-1} is used. The decays are reconstructed using the hadronic FEI and then X_c as the ROE of the $B_{\text{tag}}\ell$ system. A kinematic fit is exploited to improve the resolution and a calibration of the reconstructed q^2 is performed to take into account detector and reconstruction effects. A template fit to M_{X_c} invariant mass distribution is used to suppress the background, providing an event-by-event signal probability weight $w_i(q^2)$. The raw moments are calculated as:

$$\langle q^{2n} \rangle = \frac{\sum_i w_i(q^2) q^{2n}_{\text{cal},i}}{\sum_i w_i(q^2)} C_{\text{cal}} C_{\text{gen}},$$

where C_{cal} and C_{gen} are additional correction factors. The central moments, $\langle (q^2 - \langle q^2 \rangle)^n \rangle$, are also evaluated, given their lower correlation with the other moments. The first q^2 moment is shown in Fig. 2.

One of the great improvement of this result is the lowering of the threshold in q^2, which allows to cover 77% of the phase space. The Belle II result has been already exploited in the extraction of $|V_{cb}|$ of Ref. [13], with a better precision than the world average.

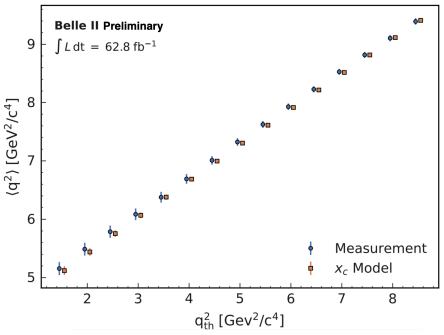

Figure 2: first q^2 moment (blue) as a function of q^2 threshold with full uncertainties. The simulated moment (orange) is shown for comparison (from Ref. [12].)

3.3. Exclusive determination of $|V_{cb}|$

In the Belle II measurement of Ref. [14] the $B^0 \to D^{*-} \ell^+ \nu$ decays are used to extract $|V_{cb}|$. A sample equivalent to an integrated luminosity of 189.3 fb^{-1} is used. The events are reconstructed using the hadronic FEI. The signal is reconstructed with the decay chain: $D^{*-} \to \overline{D}^0 \pi^-$, $\overline{D}^0 \to K^+ \pi^-$. The obtained branching fraction is: $\mathcal{B}(B^0 \to D^{*-} \ell^+ \nu) = (5.27 \pm 0.22\,(\text{stat}) \pm 0.38\,(\text{syst}))\%$.

$|V_{cb}|$ is extracted from a fit of the differential decay rate $\frac{d\Gamma}{dw} \propto \eta_{EW}^2 g(w) F^2(w) |V_{cb}|^2$, where $w = (m_B^2 + m_{D^*} - q^2_{\ell+\nu})/(2 m_B m_{D^*})$. The product of the $g(w)F^2(w)$ has been expressed with the CLN paremetrization [15] as a function of the form factors $R_1(1)$, $R_2(1)$ (as external experimental inputs), ρ^2 (free parameter) and $F(1)$ (as external lattice QCD input). The result is: $\eta_{EW} F(1) |V_{cb}| = (34.6 \pm 2.5) \cdot 10^{-3}$, $\rho^2 = 0.94 \pm 0.21$ or $|V_{cb}| = (37.9 \pm 2.7) \cdot 10^{-3}$, including both statistical and systematical uncertainties.

3.4. Exclusive determination of $|V_{ub}|$

In the Belle II measurement of Ref. [16] the $B^{+,0} \to \pi^{0,-} e^+ \nu$ decays are used to extract $|V_{ub}|$. A sample equivalent to an integrated luminosity of 189.3 fb^{-1} is used. The events are reconstructed using the hadronic FEI. The branching fraction is extracted in bins of $q^2 = (p^*_{B_{\text{sig}}} - p^*_\pi)^2$ performing a fit to the M^2_{miss} distribution. $|V_{ub}|$ is extracted from the differential decay rate $\frac{d\Gamma}{dq^2} \propto |V_{ub}|^2 f_+^2(q^2)$, where the form factor f_+ is obtained as an external lattice QCD input [17, 18]. The result is: $|V_{ub}| = (3.88 \pm 0.45) \pm 10^{-3}$, including both statistical and systematical uncertainties.

4. Unitarity triangle angles and CP violation measurements

4.1. Angular analysis of $B^+ \to \rho^0 \rho^+$

The $B^0 \to \rho\rho$ channels have a primary importance in the measurement of the α angle. The α angle is accessible through a decay-time dependent CP violation (TDCPV) analysis of $u\overline{u}d$ transition, in the interference between the $b \to u$ tree diagram transition and the decay following a flavour oscillation. The $b \to d$ penguin diagram contribution cannot be neglected and provides a $\Delta\alpha$ *penguin-pollution* phase. The penguin pollution can be estimated from an isospin analysis, the branching fraction of the involved decays and direct CPV parameter A_{CP}. The longitudinally-polarized fractions of $B \to \rho^+\rho^-$, $\rho^0\rho^0$, $\rho^+\rho^0$ channels have the lowest penguin pollution between the available decays, therefore they are the best candidates for the α measurement.

In the Belle II measurement of Ref. [19], the $B^+ \to \rho^0 \rho^+$ decays are used to measure the CP asymmetry between $B^+ \to \rho^0\rho^+$ and $B^- \to \rho^0\rho^-$ and measure the fraction of longitudinally polarized decays f_L. A sample equivalent to an integrated luminosity of 189.3 fb^{-1} is used. The ρ mesons are reconstructed using the $\rho^{0,+} \to \pi^+\pi^{-,0}$ decays. The continuum background ($e^+e^- \to q\overline{q}$) is suppressed using a Boosted Decision Tree (BDT). The branching fraction, A_{CP} and f_L

are extracted using a 6-dimensional fit, where the fitting variables are $\Delta E = E^*_B - E^*_{\text{beam}}$, the BDT output, $m_{\pi^+\pi^0}$, $m_{\pi^+\pi^-}$, and the helicity angles of the two ρ mesons. The results are:

$$f_L = 0.943^{+0.035}_{-0.033}\,(\text{stat}) \pm 0.027\,(\text{syst}),$$

$$\mathcal{B}(B^+ \to \rho^0\rho^+) = (23.2^{+2.2}_{-2.1}\,(\text{stat}) \pm 2.7\,(\text{syst})) \cdot 10^{-6},$$

$$A_{CP} = -0.069 \pm 0.068\,(\text{stat}) \pm 0.060\,(\text{syst}).$$

The latter result is not yet competitive with the world average ($A^{\text{w.a.}}_{CP} = -0.05 \pm 0.05$ [7]). However this result is only a demonstrator of the capabilities of the analysis performed on low statistics, and the precision is equivalent to the previous results scaled to the used luminosity.

4.2. Unitarity triangle angle γ determination using $B^+ \to D(K^0_S h^+ h^-)h^+$

The γ angle can be extracted from the ratio between the favored $b \to c\bar{u}s$ and the suppressed $b \to u\bar{c}s$ transition amplitudes of $B \to DK$ decays:

$$\frac{A_{\text{sup}}(B^- \to \overline{D}^0 K^-)}{A_{\text{fav}}(B^- \to D^0 K^-)} = r_B e^{i(\delta_B - \gamma)},$$

where r_B is the magnitude of the suppression while δ_B is the strong phase difference. This ratio is tree-dominated therefore the theory uncertainty is very small ($\Delta\gamma_{\text{theory}}/\gamma \sim 10^{-7}$).

The Belle II measurement of Ref. [20] adopts the BPGGSZ formalism [21–23], and uses two self-conjugated D^0 decays: $D^0 \to K^0_S\pi^+\pi^-$ and $D^0 \to K^0_S K^+ K^-$. The Belle II sample equivalent to an integrated luminosity of 128 fb^{-1} plus the entire Belle sample (711 fb^{-1}) are used. The analysis is performed binned in the Dalitz space of $K_S h^\pm$ to be independent from the D^0 decay model. The strong phase is obtained from CLEO and BES III experiments measurements [24–26]. The backgrounds are suppressed with a BDT. The event yields are obtained from a simultaneous fit of the signal and the control sample $B^+ \to D^0(\to K_S h^+ h^-)\pi^+$, used to constraint the fraction of events in each Dalitz bin. The fit is performed in two dimensions: ΔE and the output of the BDT. The result is:

$$\gamma = (78.4 \pm 11.4\,(\text{stat}) \pm 0.5\,(\text{syst}) \pm 1.0\,(\text{ext.inp.}))^\circ,$$

where the world average is $\gamma^{\text{w.a.}} = (65.9^{+3.3}_{-3.5})^\circ$ [7].

4.3. B^0 lifetime and mixing frequency

The B^0 lifetime τ_{B^0} and mixing frequency Δm_d are two central ingredients to perform TDCPV analyses. In the Belle II measurement of Ref. [27] they are measured using an inclusive B-tagging method. A sample equivalent to an integrated luminosity of 190 fb^{-1} is used. The signal is reconstructed in $B \to D^{(*)-}\pi^+$ and $B \to D^{(*)-}K^+$ modes. The B_{tag} is identified using the ROE tracks. After the reconstruction of the two B mesons, the Belle II flavour tagger algorithm is used to define same flavour (an event that experiences the $B^0 - \overline{B}^0$ mixing) and opposite flavour categories (an event that did not experienced $B^0 - \overline{B}^0$ mixing). The backgrounds are suppressed with a BDT. The decay time difference Δt is fitted with a model which includes the effects of wrong tagging and vertex resolution effects. The results are:

$$\tau_{B^0} = 1.499 \pm 0.013\,(\text{stat}) \pm 0.008\,(\text{syst})\ \text{ps},$$

$$\Delta m_d = 0.516 \pm 0.008\,(\text{stat}) \pm 0.005\,(\text{syst})\ \text{ps}^{-1}.$$

The results are not yet competitive compared with the world average ($\tau^{\text{w.a.}}_{B^0} = 1.510 \pm 0.004$ ps, $\Delta m^{\text{w.a.}}_d = 0.50665 \pm 0.0019$ ps^{-1}). However the systematic uncertanties are reduced compared to previous measurements and an extension with the semileptonic channels and more statistic can easily improve the precision.

4.4. Time dependent analysis of $B^0 \to K^0_S\pi^0$

The $B^0 \to K^0_S\pi^0$ is a particularly interesting channel because it is generated from the $b \to s\bar{d}\bar{d}$ loop transition, suppressed in the SM. Therefore it is a natural candidate for BSM searches. Belle II has a unique reach in this channel, given the fully neutral light mesons final state. Since $K^0_S\pi^0$ is a CP eigenstate, the time-dependent decay rate allows to extract both the direct CP-violation amplitude (A_{CP}) and the CP-violation amplitude in the interference between the direct amplitude and the amplitude of the decay following a flavor oscillation (S_{CP}):

$$P(\Delta t) = \frac{e^{-|\Delta t|/\tau_{B^0}}}{4\tau_{B^0}} \{1 + q[A_{CP}\cos(\Delta m_d \Delta t) + S_{CP}\sin(\Delta m_d \Delta t)]\},$$

where q is the sign of the charge of the b quark in the B_{tag}. The SM expectations are $A_{CP} \simeq 0$ and $S_{CP} \simeq \sin 2\beta$.

Moreover, the study of A_{CP} in this channel is crucial because of the so-called $K\pi$-puzzle. In Ref. [28] is presented an isospin sum rule $I_{K\pi}$, expected to be 0 with a 1% precision in the SM. Experimentally $I_{K\pi} = -0.11 \pm 0.13$ with the main uncertainty coming from $A_{CP}^{K^0_S\pi^0}$. More details can be found in Ref. [29].

The $B^0 \to K^0_S\pi^0$ branching fraction and A_{CP} are measured by Belle II in Ref. [30]. A sample equivalent to an integrated luminosity of 189.8 fb^{-1} is used. Given the limited statistical power of the sample S_{CP} is kept fixed to previous measured value in the fit. The decay is reconstructed using $K^0_S \to \pi^+\pi^-$, $\pi^0 \to \gamma\gamma$

channels, a dedicated K^0_S vertex fit is exploited and the Belle II flavour tagger is used to define the B^0 and $\overline{B}^0$ categories. An extended maximum likelihood fit is performed in four dimensions: ΔE, M'_{bc}, Δt and the output of the BDT for background suppression (where $M'^2_{bc} = E^2_{\rm beam} - \left[\vec{p}_K + \vec{p}_\pi/|\vec{p}_\pi| \sqrt{(E_{\rm beam} - E_K)^2 - m^2_\pi}\right]^2$). The results are:

$A_{CP} = -0.41^{+0.30}_{-0.32}\,(\text{stat}) \pm 0.09\,(\text{syst})$,

$\mathcal{B}(B^0 \to K^0_S\pi^0) = (11.0 \pm 1.2\,(\text{stat}) \pm 1.0\,(\text{syst})) \cdot 10^{-6}$,

where the world average are $A^{\text{w.a.}}_{CP} = -0.01 \pm 0.10$ and $\mathcal{B}(B^0 \to K^0_S\pi^0)^{\text{w.a.}} = (9.9 \pm 0.5) \cdot 10^{-6}$ [7].

5. Rare B decays

Decays which involve $b \to s$ transitions are flavour changing neutral currents which are suppressed in the SM. The SM branching fractions are $O(10^{-5} - 10^{-7})$, predicted with large uncertainties (10 – 30%). However combinations of amplitudes (ratios, asymmetries, angular distributions...) can improve the precision on specific observables. This sector offers also the possiblity to test lepton flavour universality and perform searches for lepton flavor violation. Most of the interesting channels will become competitive with an integrated luminosity of few ab^{-1}, while now being statistically limited. However, Belle II has a unique reach in several channels of this sector, given the good performance both in electron and muon reconstruction and the capabilities of performing precise measurements also with multiple neutrinos, photons and neutrals in the final state.

5.1. Branching fraction of $B \to K^*\ell^+\ell^-$

The Belle II analysis of Ref. [31] performed the measurement of $\mathcal{B}(B \to K^*\ell^+\ell^-)$, where $\ell = e, \mu$, $K^* = K^{*+}(892)$, $K^{*0}(892)$. This is a first step towards the measurement of $R_{K^{(*)}}$, which currently shows a discrepancy of 2-3σ with the SM predictions [7, 32]. A sample equivalent to an integrated luminosity of 189 fb^{-1} is used. The K^* is reconstructed combining a kaon (K^+ or K^0_S) and pion (π^- or π^0). A BDT is used to suppress the backgrounds. A veto on the dilepton invariant mass is applied for the $J/\psi, \psi(2S) \to \ell\ell$ background. An extended maximum likelihood fit is performed to the 2-dimensional $(\Delta E, M_{bc})$ distribution, where $M^2_{bc} = E^{*2}_{\rm beam} - p^{*2}_B$. The results are:

$\mathcal{B}(B \to K^*\mu^+\mu^-) = (1.19 \pm 0.31\,(\text{stat})^{+0.08}_{-0.07}\,(\text{syst})) \cdot 10^{-6}$,

$\mathcal{B}(B \to K^*e^+e^-) = (1.42 \pm 0.48\,(\text{stat}) \pm 0.09\,(\text{syst})) \cdot 10^{-6}$,

$\mathcal{B}(B \to K^*\ell^+\ell^-) = (1.25 \pm 0.30\,(\text{stat})^{+0.08}_{-0.07}\,(\text{syst})) \cdot 10^{-6}$,

where the world average are $(1.06 \pm 0.09) \cdot 10^{-6}$, $(1.19 \pm 0.20) \cdot 10^{-6}$,$(1.05 \pm 0.1) \cdot 10^{-6}$, respectively [7].

5.2. Search for $B^+ \to K^+\nu\overline{\nu}$ decays

The search of $B^+ \to K^+\nu\overline{\nu}$ decay is a unique opportunity for Belle II. The measurement of Ref. [33] is performed on a sample equivalent to an integrated luminosity of 63 fb^{-1}. The reconstruction is performed using the inclusive tagging, thus reconstructing the $B_{\rm sig}$ using the highest p_T track compatible with a K^+, and then assigning the entire ROE to the $B_{\rm tag}$. The procedure is validated on $B^+ \to J/\psi(\to \mu\mu)K^+$ decays. A pair of BDT in cascade are used to fully exploit the event information to suppress the backgrounds.

No signal is observed and the result is expressed in term of upper limit using the CL$_s$ method [34]. The expected upper limit on $B^+ \to K^+\nu\overline{\nu}$ is $2.3 \cdot 10^{-5}$ at the 90% C.L in background only hypothesis. The observed upper limit is $4.1 \cdot 10^{-5}$ at the 90% C.L. This results is also recasted in term of signal strength or $\mathcal{B}(B^+ \to K^+\nu\overline{\nu}) = (1.9 \pm 1.3\,(\text{stat})^{+0.08}_{-0.07}\,(\text{syst})) \cdot 10^{-5}$, compatible with the SM prediction and the previous results [7]. The Belle II plan is to extend this measurement with a larger sample and additional channels (K^*, K^0_S).

6. Dark sector: dark Higgs-strahlung

The BSM searches in the dark sector are an important part of the Belle II physics program and an opportunity to exploit the initial data samples. Belle II has a unique reach in light dark matter in the MeV to GeV scale. The hermetic detector, the clean events and the dedicated low-multiplicity triggers create an optimal environment for these searches.

One of the lastest Belle II results in this sector is the search presented in Ref. [35]. A sample equivalent to an integrated luminosity of 8.34 fb^{-1} is used. This analysis relies on a specific model which expects a dark photon (A') mixed with a SM γ. The A' mass is generated by a spontaneous symmetry breaking mechanism induced by a dark higgs h'. The latter has no SM coupling. Requiring the specific mass hierarchy $m_{h'} < m_{A'}$ the h' is emitted via Higg-strahlung and it is long-lived and undetected, while the decay $A' \to \mu^+\mu^-$ is favored. This particular configuration is chosen because it is mostly unexplored compared to other already investigated mass hierarchies. The analysis is perfomed with a scan of the $M_{\mu\mu} \times M_{\rm rec}$ plane, where $M_{\rm rec}$ is the recoil against the dimuon system. No excess is found but the the world best upper limit at 90% C.L. is set for 1.65 GeV $< m_{A'} <$ 10.51 GeV. In Fig. 3 the upper limit distribution on the $m_{h'} \times m_{A'}$ plane is shown.

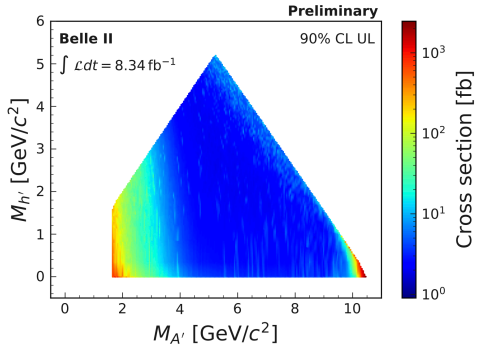

Figure 3: Observed 90% CL upper limit on the cross section $e^+e^- \to A'h'$ with $A' \to \mu^+\mu^-$ and h' invisible as a function of the A' and h' masses. Values are computed at search window centers and then interpolated to points of the search plane (from Ref. [35]).

7. Conclusion and prospects

The Belle II measurements presented here span a large part of the physics program of the experiment. Most of them are statistically limited, showing that the systematic uncertainties, and thus the calibration of the experimental apparatus, are under control. The Long Shutdown 1 started at the end of June 2022, required for several upgraded of the collider and the detector. All the presented measurements will be repeated soon with the larger data sample collected until the Long Shutdown 1. However, several results will became competitive only with 2-4 ab^{-1}, but they already demonstrates the capabilities of the experiment in term of performance and novel analysis techniques.

References

[1] Belle II collaboration, Belle II Technical Design Report (2010). arXiv:1011.0352.

[2] K. Akai, K. Furukawa, H. Koiso, SuperKEKB collider, Nucl. Instrum. Methods Phys. Res. Sect A 907 (2018) 188–199.

[3] BABAR collaboration, The BABAR detector, Nucl. Instrum. Meth. Phys. Res. Sect A 479 (1) (2002) 1–116.

[4] B. collaboration, The Belle detector, Nucl. Instrum. Meth. Phys. Res. Sect A 479 (1) (2002) 117–232.

[5] M. Neubert, B decays and the heavy quark expansion, Adv. Ser. Direct. High Energy Phys. 15 (1998) 239–293.

[6] Belle II collaboration, Precise measurement of the D^0 and D^+ lifetimes at Belle II, Phys. Rev. Lett. 127 (2021) 211801.

[7] R. L. Workman et al. (Particle Data Group), Review of Particle Physics, PTEP 2022 (2022) 083C01.

[8] Belle II collaboration, Measurement of the Λ_c^+ lifetime (2022). arXiv:2206.15227.

[9] Y. Amhis et al. (HFLAV group), Averages of b-hadron, c-hadron, and τ-lepton properties as of 2021 (2022). arXiv:2206.07501.

[10] T. Keck et al., The full event interpretation, Comput. Sofw. Big Sci. 3 (1) (2019) 6.

[11] M. Fael, T. Mannel, K. Keri Vos, V_{cb} determination from inclusive $b \to c$ decays: an alternative method, JHEP 02 (2019) 177.

[12] Belle II collaboration, Measurement of Lepton Mass Squared Moments in $B \to X_c \ell \bar{\nu}_\ell$ Decays with the Belle II Experiment (2022). arXiv:2205.06372.

[13] F. Bernlochner et al., First extraction of inclusive V_{cb} from q^2 moments (2022). arXiv:2205.10274.

[14] W. Sutcliffe (Belle II collaboration), Semileptonic B decays, BELLE2-TALK-CONF-2022-032.

[15] I. Caprini, L. Lellouch, M. Neubert, Dispersive bounds on the shape of $B \to D^* \ell\nu$ form factors, Nucl. Phys. B 530 (1) (1998) 153–181.

[16] Belle II collaboration, Study of Exclusive $B \to \pi e^+ \nu_e$ Decays with Hadronic Full-event-interpretation Tagging in 189.3 fb^{-1} of Belle II Data (2022). arXiv:2206.08102.

[17] J. Bailey et al., $|V_{ub}|$ from $B \to \pi\ell\nu$ decays and (2 + 1)-flavor lattice QCD, Phys. Rev. D 92 (2015) 014024.

[18] C. Bourrely, L. Lellouch, I. Caprini, Model-independent description of $B \to \pi l\nu$ decays and a determination of $|V_{ub}|$, Phys. Rev. D 79 (2009) 013008.

[19] Belle II collaboration, Angular analysis of $B^+ \to \rho^+\rho^0$ decays reconstructed in 2019, 2020, and 2021 Belle II data (2022). arXiv:2206.12362.

[20] Belle and Belle II collaborations, Combined analysis of Belle and Belle II data to determine the CKM angle ϕ_3 using $B^+ \to D(K^0_S h^- h^+)h^+$ decays, JHEP 02 (2022) 063. arXiv:2110.12125.

[21] A. Bondar, Proceedings of BINP special analysis meeting on Dalitz analysis, unpublished (2002).

[22] A. Giri, Y. Grossman, A. Soffer, J. Zupan, Determining γ using $B^\pm \to \mathrm{dk}^\pm$ with multibody d decays, Phys. Rev. D 68 (2003) 054018.

[23] B. collaboration, Measurement of ϕ_3 with dalitz plot analysis of $B^\pm \to D^{(*)}K^\pm$ decay, Phys. Rev. D 70 (2004) 072003.

[24] CLEO collaboration, Model-independent determination of the strong-phase difference between D^0 and $\overline{D}^0 \to K^0_{S,L} h^+ h^-$ ($h = \pi, K$) and its impact on the measurement of the CKM angle γ/ϕ_3, Phys. Rev. D 82 (2010) 112006.

[25] BESIII collaboration, Model-independent determination of the relative strong-phase difference between D^0 and $\overline{D}^0 \to K^0_{S,L}\pi^+\pi^-$ and its impact on the measurement of the CKM angle γ/ϕ_3, Phys. Rev. D 101 (2020) 112002.

[26] BESIII collaboration, Improved model-independent determination of the strong-phase difference between D^0 and $\overline{D}^0 \to K^0_{S,L} K^+ K^-$ decays, Phys. Rev. D 102 (2020) 052008.

[27] T. Humair (Belle II collaboration), Time-dependent cp violation and charmless decays, BELLE2-TALK-CONF-2022-031 (2022).

[28] M. Gronau, A precise sum rule among four $B \to K\pi$ CP asymmetries, Phys. Lett. B 627 (1) (2005) 82–88.

[29] R. Fleischer, R. Jaarsma, E. Malami, K. K. Vos, Exploring $B \to \pi\pi, \pi K$ decays at the high-precision frontier, Eur. Phys. J. C 78 (11) (2018) 943. arXiv:1806.08783.

[30] Belle II collaboration, First decay-time-dependent analysis of $B^0 \to K^0_S \pi^0$ at Belle II (2022). arXiv:2206.07453.

[31] Belle II collaboration, Measurement of the branching fraction for the decay $B \to K^*(892)\ell^+\ell^-$ at Belle II (2022). arXiv:2206.05946.

[32] LHCb collaboration, Test of lepton universality in beauty-quark decays, Nature Phys. 18 (3) (2022) 277–282. arXiv:2103.11769.

[33] Search for $B^+ \to K^+\nu\bar{\nu}$ Decays Using an Inclusive Tagging Method at Belle II, Phys. Rev. Lett. 127 (2021) 181802.

[34] A. L. Read, Presentation of search results: the CL$_s$ technique, J. Phys. G: Nucl. Part. Phys. 28 (10) (2002) 2693–2704.

[35] Belle II collaboration, Search for a dark photon and an invisible dark Higgs boson in $\mu^+\mu^-$ and missing energy final states with the Belle II experiment (2022). arXiv:2207.00509.